AIP Advances

Experimental investigation of the particle oscillation instability in a single-axis acoustic levitator

Cite as: AIP Advances **9**, 035020 (2019); https://doi.org/10.1063/1.5078948
Submitted: 29 October 2018 . Accepted: 28 February 2019 . Published Online: 14 March 2019

Marco A. B. Andrade, Spyros Polychronopoulos, Gianluca Memoli, and Asier Marzo

Experimental investigation of the particle oscillation instability in a single-axis acoustic levitator

Cite as: AIP Advances 9, 035020 (2019); doi: 10.1063/1.5078948
Submitted: 29 October 2018 • Accepted: 28 February 2019 •
Published Online: 14 March 2019

Marco A. B. Andrade,[1,a)] Spyros Polychronopoulos,[2] Gianluca Memoli,[3] and Asier Marzo[4]

AFFILIATIONS

[1]Institute of Physics, University of São Paulo, São Paulo 05508-090, Brazil
[2]Informatics and Telecommunications, National and Kapodistrian University of Athens, Athens 15784, Greece
[3]School of Engineering and Informatics, University of Sussex, Brighton BN1 9RH, UK
[4]Computer Science, Public University of Navarre, Pamplona 31006, Navarre, Spain

[a)]**Author to whom correspondence should be addressed. Electronic mail:** marcobrizzotti@gmail.com

ABSTRACT

Single-axis acoustic levitators are employed in biomedicine, chemistry and physics experiments due to their ability to trap in mid-air objects of a wide range of materials and sizes. Although this type of levitator has been studied for decades, there are effects that are not well understood. One of these effects is the particle oscillation instability, in which the levitating particle starts to oscillate with increasing amplitude until it is ejected out of the levitator. Most of the operations performed with acoustic levitation require high accuracy regarding the positioning of the particle, thus a lack of stability severely hinders the experiments. In this paper, we present an experimental setup that consists of a single-axis levitator, a mechanized stage to control the separation between the emitter and the reflector, a scale to measure the radiation force and a high-speed camera. We experimentally investigate the effect of the distance between the emitter and the reflector on the apparatus resonant frequency and on levitation stability. In accordance with previous theoretical studies, three types of levitation behavior were experimentally identified: stable levitation, oscillation of constant amplitude and unstable oscillation. We also show that the type of levitation behavior can be controlled by changing the distance between the emitter and the reflector.

I. INTRODUCTION

Acoustic levitation[1,2] uses the radiation force[3] generated by sound waves to suspend liquids[4,5] and solids[6] in mid-air. This method has been used in a wide range of applications, such as chemical analysis of levitated samples,[7,8] trapping heavy gases,[9] measuring the surface tension of liquids,[10,11] amorphous drugs production,[12] and structural characterization of proteins.[13] Acoustic levitation has even been employed to levitate living insects,[14] soap bubbles,[15] and food.[16]

There are various types of acoustic levitators.[17–21] The most commonly used and studied one is the single-axis levitator which consists of an emitter and an opposing reflector,[22–26] or two opposing emitters.[27,28] In this type of levitator, a standing wave is formed between the two opposed elements and particles can be trapped at the pressure nodes.[3]

Acoustic levitation offers several advantages over optical[29] or magnetic levitation,[30] e.g. high ratio of trapping force to input power, capability of levitating a wide range of materials as well as sample sizes, and low-cost apparatus.[28] Due to the aforementioned advantages, extensive research has been conducted on acoustic levitation[2] to enhance the manipulation of the levitated particle in one,[31,32] two,[33,34] and three dimensions.[20,35–38] Despite the recent advances, one of the key remaining issues is the stability of the levitated object.

The levitated object is regularly perturbed by small air currents or acoustic streaming.[39,40] In general, these perturbations are small and do not significantly affect the levitation.[41,42] When the

object is displaced from its equilibrium point, the converging acoustic radiation forces act as a spring and the surrounding air generates a drag force, causing a damped oscillatory motion that drags the particle towards its equilibrium position.[43] However, in some occasions, small perturbations lead to instability and the oscillation amplitude increases exponentially over time. In these cases the object either oscillates with a large constant amplitude or hits the levitator's walls.[44–47] The stable levitation of a sphere and the same sphere oscillating vertically with constant amplitude are shown in Fig. 1(a) and Fig. 1(b), respectively.

Oscillational instabilities can negatively affect measurements,[8] hindering expensive experiments or leading to the loss of valuable samples. For example, the contactless acoustic positioning of a molten glass sample aboard the Challenger space shuttle (Mission STS-41B, 1984) failed because the sample oscillated with increasing amplitude until it hit the chamber's wall.[44,48] Two decades later, the self-excited oscillation of liquid drops in a single-axis acoustic levitator was reported,[49] in which a slow raise of the vertical amplitude oscillation was followed by non-axisymmetric sectorial oscillations.

A theoretical analysis of the oscillational instability was firstly presented by Rudnick and Barmatz.[44] They observed that (a) the presence of a levitated object in the levitator affects its resonance frequency[50,51] and (b) a phase difference exists between the speed of the oscillating particle and the driving frequency. These two factors result in a (time-averaged) velocity-dependent term in the equation of the particle motion, i.e. a damping factor whose sign depends on whether the driving frequency is above or below the levitator's resonance frequency. For driving frequencies greater than the levitator's resonance, this additional damping term is negative and causes the exponential increase of the amplitude of the oscillating object. In some cases, the oscillation stabilizes at a certain amplitude, but in others, the amplitude increases until the object hits the levitator's walls or gets ejected.

Although Rudnick and Barmatz[44] theoretically investigated the oscillational instability almost three decades ago, few experimental studies[45,46] have been conducted to test their main conclusions. Therefore, the main objective of this study is to experimentally investigate the oscillational instability and identify the conditions that lead to stable levitation or vertical oscillations based on the distance between the transducer and the reflector. In this paper, we experimentally investigate the oscillational instability of a single-axis acoustic levitator consisting of a planar transducer and an opposing planar reflector. The levitated sphere oscillations were captured with a high-speed camera and a tracking algorithm was used to obtain the sphere's vertical position as a function of time. In addition, an electronic scale was used to measure the acoustic radiation force on the reflector as a function of the distance between the transducer and the reflector.

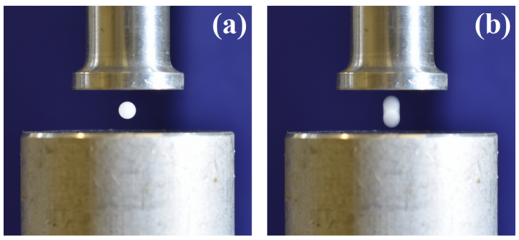

FIG. 1. Acoustic levitation of a polypropylene sphere of 3 mm in diameter: (a) Stable levitation; (b) Oscillational instability.

II. SIMPLE ANALYTICAL MODEL

The acoustic radiation force on a small object located in the area of a pressure node can be approximated by the restoring force of a spring.[2,43,52] Neglecting gravity and assuming a Stokes' drag force, the vertical oscillation of the levitating object can be described by a damped harmonic oscillator,[53] whose motion equation is given by

$$m\frac{d^2z}{dt^2} + R\frac{dz}{dt} + kz = 0, \tag{1}$$

where z is the vertical position of the levitated object, m is the object's mass, R is the viscous damping coefficient and k is the elastic constant, which is proportional to the square of the acoustic pressure's amplitude in the levitator.[43] Considering Eq. (1), an object displaced from its equilibrium position would oscillate with a decreasing amplitude until it reaches the equilibrium position. However, the strength of the trapping force changes with the object position because the displacement of the levitated object changes the levitator's resonance frequency.[44,50,51] Due to the response time of the acoustic levitator, the object's velocity also affects the trapping force.[44,53] Primarily, this force is not in phase with the object's velocity and leads to one of the following three scenarios: 1) The velocity's dependent term acts as a damping force that increases the total damping coefficient R. 2) The velocity's dependent term increases the oscillation's amplitude until a saturation state is reached (in this case we can assume $R = 0$). 3) The oscillation's amplitude increases exponentially until the object hits the levitator walls ($R<0$).

III. EXPERIMENTAL SETUP

The single-axis acoustic levitator consists of: a homemade 25 kHz Langevin transducer with a planar radiating face of 20 mm in diameter, and an opposing plane reflector of 38 mm in diameter. The reflector is placed at a distance H from the transducer. In all the experiments, the transducer emitted a sinusoidal wave of 25.25 kHz, and the levitator operated under the first mode ($H \approx \lambda/2$), with λ being the acoustic wavelength ($\lambda = 13.58$ mm). This apparatus creates a standing wave where a small sphere can levitate at the pressure node.

The oscillational instability was investigated using the experimental setup shown in Fig. 2. The position of the levitated object was captured with a high-speed camera (Photron FASTCAM Mini UX50). An electronic scale (Shimadzu UX420H, Kyoto, Japan), with a resolution of 0.001 g, was placed below the reflector to measure the radiation force acting on it. The radiation force on the reflector is proportional to the square of the acoustic pressure amplitude and it is maximum at the resonance states of the acoustic cavity. The transducer was attached to a vertical motorized linear stage (Thorlabs NRT150/M) with an accuracy of 2 μm and minimum increment of 0.1 μm. The stage and the scale were both controlled by a MATLAB script, allowing the measurement of the acoustic radiation force on the reflector for various distances (H) between the reflector and

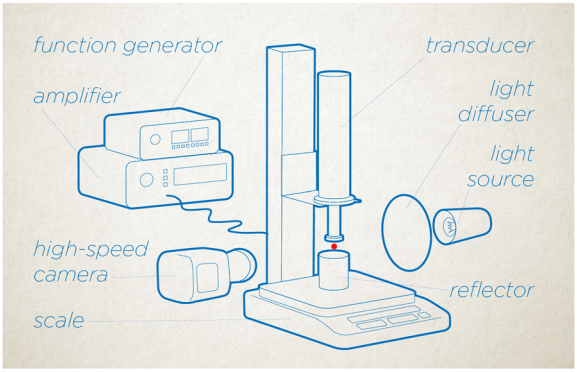

FIG. 2. The experimental setup. The reflector sits on top of a scale that measures the acoustic radiation force acting on it. A transducer is mounted on a motorize stage to accurately control the distance to the reflector. A function generator creates the driving signal that gets amplified and fed to the transducer. Diffuse illumination is opposite a high-speed camera that captures the particle's position.

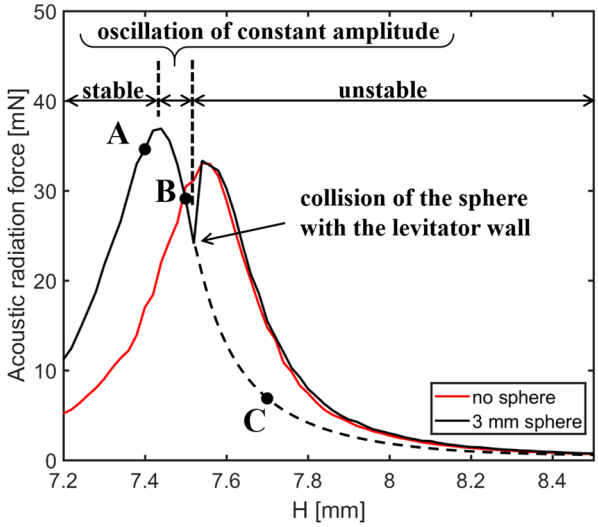

FIG. 3. Acoustic radiation force on the reflector as a function of the distance between the emitter and the reflector (H), with and without the levitated sphere. Points A, B and C are respectively within the regions of stable levitation, oscillation with constant amplitude, and oscillation with increasing amplitude. In our experiment, the 3 mm sphere (red curve) collided with the reflector at H = 7.52 mm. Right after the sphere was removed from the levitator, the force matched the black curve for $H > 7.52$ mm.

the transducer. The acoustic radiation force was measured with and without the presence of the levitated object in the levitator. The levitated object was a polypropylene (density 875 kg/m^3) sphere of 3 mm in diameter. The transducer's input signal was generated by a Keysight 33512B function generator and amplified by a high-power amplifier (700A1, Amplifier Research Corp., Souderton, PA).

Small temperature variations occurred during the operation of the transducer, affecting its displacement's amplitude. To overcome these fluctuations during the experiment, a small piezoceramic was bonded on the transducer's rear face to monitor its performance. The transducer's voltage amplitude was controlled to make the piezoceramic's voltage stable during the measurements.

IV. RESULTS AND DISCUSSION

The first set of measurements was taken without the sphere in the levitator. By assuming a plane wave radiation, the first resonance should be at $H = \lambda/2$ (6.79 mm) with the speed of sound in the air medium being c = 343 m/s. However, as can be seen in Fig. 3, the largest acoustic radiation force occurs at $H \approx 7.55$ mm. This result is in agreement with Xie's and Wei's work,[6] where they showed that in a typical single-axis acoustic levitator the first resonance occurs when H is slightly greater than $\lambda/2$.

For the second set of measurements, we introduced a 3 mm polypropylene sphere in the levitator and the force acting on the reflector was captured for various distances H (from 7.20 mm to 8.50 mm in 0.02 mm steps). The sphere levitated stably for distances between H = 7.20 and 7.42 mm. When the distance reached $H \approx 7.44$ mm, the sphere started to oscillate vertically with constant amplitude and frequency. For distances between $H \approx 7.44$ and 7.52 mm, the amplitude of the oscillatory motion increased monotonically, until the sphere collided with the reflector at H = 7.52 mm. At this point, the sphere was removed from the levitator, making the black and red curves of Fig. 3 coincide. For $H > 7.52$ mm the levitation was not stable, i.e. the amplitude of the vertical oscillation increased over time, until the sphere collided with the levitator. The dashed black line of Fig. 3 represents the expected force if we could measure the force with the sphere inside.

As can be seen in Fig. 3, the presence of an object inside the levitator causes a shift of the resonance frequency.[44,50,51] When the sphere is introduced in the levitator, the acoustic radiation peak shifts from $H \approx 7.55$ mm to $H \approx 7.44$ mm.

This change is in line with the theory presented by Curzon,[51] and Rudnick and Barmatz[44] which, adapted to the case of a single-axis levitator driven at a fixed frequency ω_0 (height H, diameter D, unperturbed pressure field $p(z) = A_0 \cos(k_0 z)$, with $k_0 = n\pi/H$ and $n = 1, 2, 3, \ldots$) gives:

$$\frac{\Delta\omega}{\omega_0} = 2\frac{V_p}{V_c}\left(\frac{5}{2}\cos^2(k_0 z) - \frac{3}{2}\right), \tag{2}$$

where z is the vertical position of the levitated particle in the levitator, V_p is the volume of the levitated object (i.e. $\frac{4}{3}\pi a^3$ in the case of a sphere of radius a) and V_c is the volume in the levitator not occupied by the particle. Assuming H = 7.55 mm, D = 20 mm, f_0 = 25.25 kHz (k_0 = 462.54 m^{-1}) and a 3 mm in diameter particle positioned at $H/2$, equation (2) gives a theoretical frequency shift $\Delta\omega/\omega_0 = -0.0171$, which is in good agreement with our experimental measurement ($\Delta\omega/\omega_0 = -0.0148$). A possible reason for the discrepancy is that, according to the theory, the particle levitates slightly below the pressure node, i.e. its equilibrium position is no longer at $H/2$. In addition, Eq. (2) was proposed for a closed chamber whereas in our experiments we used an open levitator.

We classify the levitation behavior in three types: stable (H = 7.20-7.44 mm), oscillation of constant amplitude ($H \approx$ 7.44-7.52 mm) and unstable oscillation (H = 7.52-8.50 mm). These

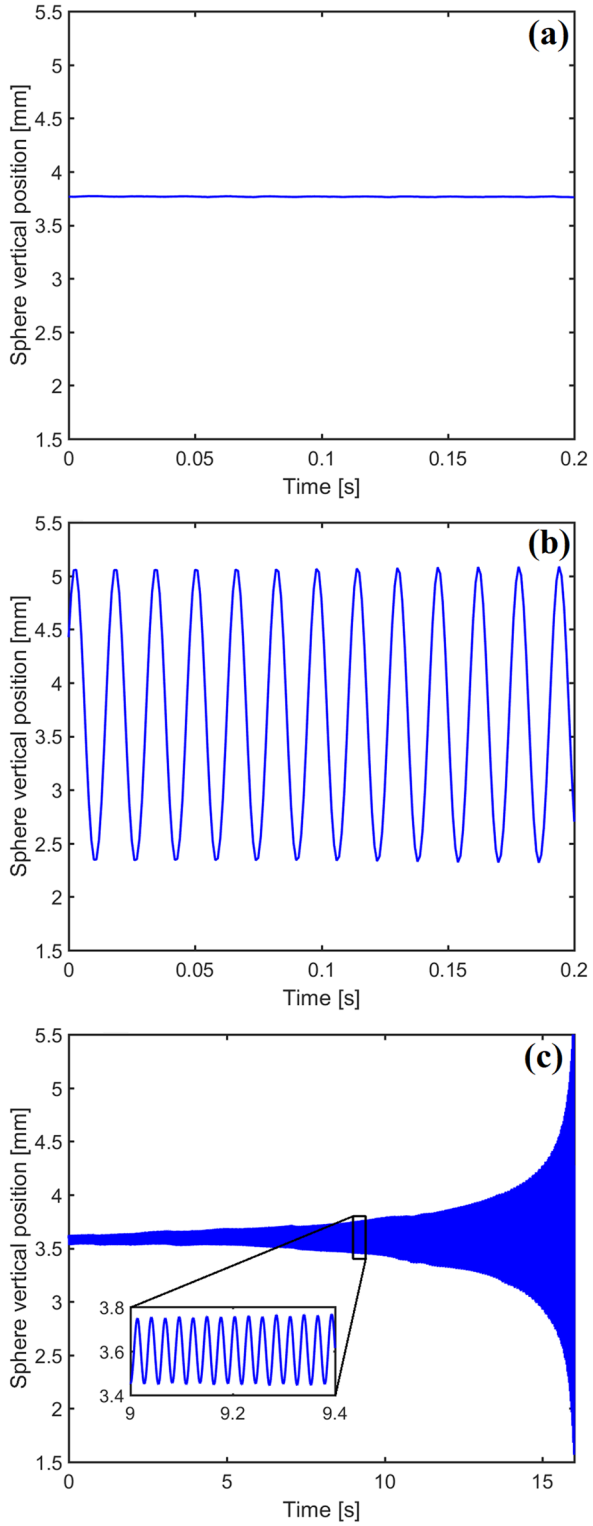

FIG. 4. Vertical position of the sphere over time for the three points of Fig. 3. (a) Point A - Stable levitation (H = 7.4 mm). (b) Point B - Oscillation of constant amplitude (H = 7.5 mm). (c) Point C - unstable oscillation (H = 7.7 mm).

types of motion can be seen in supplementary material video 1. The sphere's vertical position over time for points A, B and C from Fig. 3 are presented in Fig. 4. In Fig. 4(a), the transducer separation was H = 7.4 mm and the sphere levitated stably at z = 3.76 mm. When H was increased to 7.5 mm [see Fig. 4(b)], the sphere oscillated with a constant amplitude of 2.7 mm (peak-to-peak) at a frequency of 62 Hz. For H = 7.7 mm [see Fig. 4(c)], the oscillation's amplitude increased over time until the object hits the reflector.

The results of Fig. 4 can be interpreted by making an analogy with a damped harmonic oscillator. When the levitation is stable [Fig. 4(a)], we can assume that the damping parameter R is positive. In this situation, if an external perturbation displaces the particle from its equilibrium position, a damped oscillatory motion is expected. To illustrate this behavior, the distance between the transducer and the reflector was set to H = 7.4 mm (stable levitation) and transducer voltage amplitude was reduced to one third of the original value, causing the levitation height to decrease from z = 3.76 mm to 3.41 mm (Fig. 5). Then, at t = 0.32 s, the voltage amplitude was changed to its original value, causing the sphere equilibrium position to change to z = 3.76 mm and inducing the damped oscillatory motion of the sphere, as it can be seen in Fig. 5.

In some conditions, as illustrated in Fig. 4(b), the viscous drag force on the sphere can be neutralized by the action of a velocity-dependent term caused by the time delay in the levitator's response.[44] In this situation, the oscillation amplitude increases until a saturation state is reached, causing the sphere to oscillate with constant amplitude. This oscillatory motion can be described by assuming R = 0, in which the motion equation takes the form of an undamped harmonic oscillator. In our experiment, the oscillations with constant amplitude occur for H varying between 7.44 and 7.52 mm. This type of oscillation was captured by the high-speed camera (see supplementary material video 2) and is summarized in Fig. 6, which illustrates the peak-to-peak amplitude of the

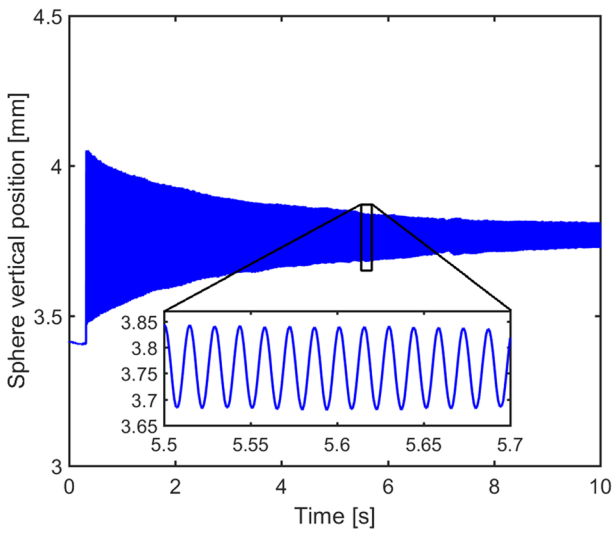

FIG. 5. Damped oscillation of the levitated sphere for H = 7.4 mm.

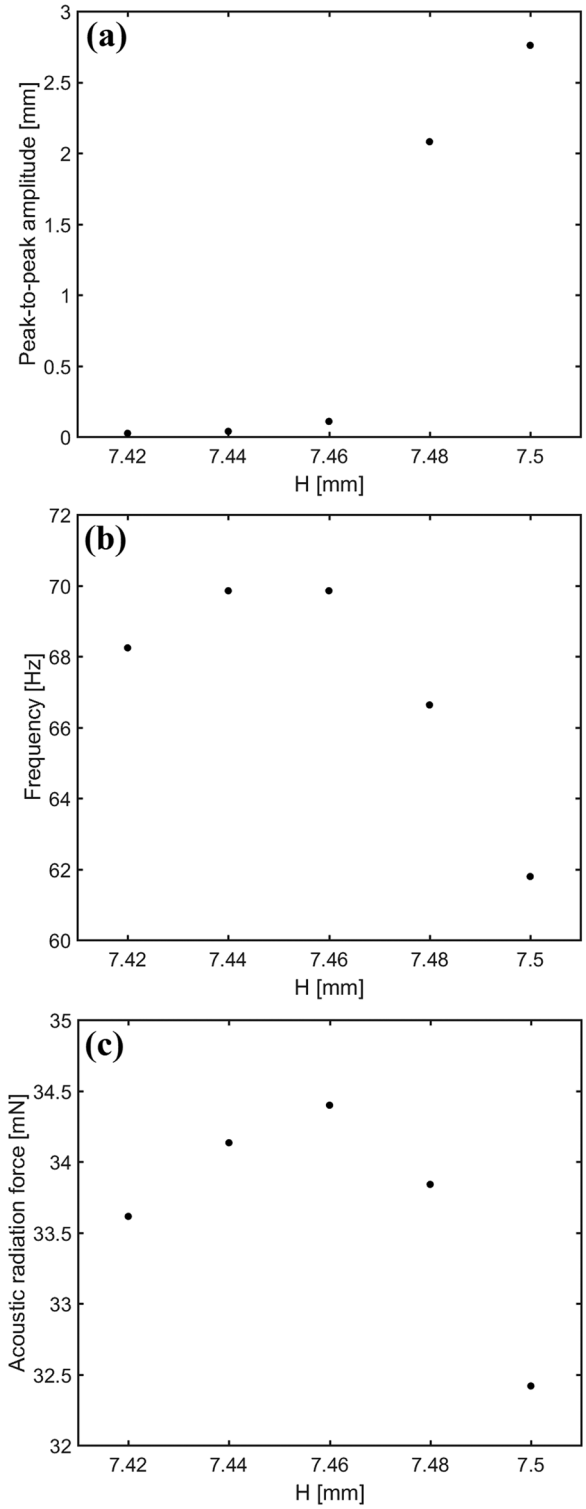

FIG. 6. Peak-to-peak amplitude of the particle oscillations (a), oscillation frequency (b), and radiation force on the reflector (c) as a function of H for the sphere oscillating with constant amplitude. The resonance in presence of the particle is at H = 7.44 mm.

vertical oscillations [Fig. 6(a)], the oscillation frequency [Fig. 6(b)] and the acoustic radiation force on the reflector [Fig. 6(c)] as a function of H. In this range *of* H, the oscillation amplitude increases monotonically with H, while the oscillation frequency reached a maximum around $H \approx 7.45$ mm, which coincides with the peak of the force curve [Figs. 3 and 6(c)]. This increase in the oscillation frequency at the resonance can be explained by the elastic constant k. The trapping elastic constant k scales with the square of the acoustic pressure amplitude.[2,43] At the resonance, the acoustic pressure gets maximized, leading to a maximum oscillation frequency.

The unstable levitation shown in Fig. 4(c) is characterized by a negative damping constant ($R < 0$). In this condition the solution of Eq. (1) predicts that the oscillation's amplitude will increase exponentially over time. This prediction is in agreement with our experimental results as shown in Fig. 4(c).

The experimental results presented in this paper show that stable levitation can be achieved when the distance between the emitter and the reflector is less than the resonance distance in the presence of an object ($H \approx 7.44$ mm $\approx 0.547\lambda$). When the distance is marginally greater than $H \approx 7.44$ mm, the object oscillates vertically with constant amplitude. For $H > 0.554\lambda \approx 7.52$ mm, the levitation becomes unstable and the oscillation's amplitude increases exponentially over time, until the object collides with the levitator walls. Our experiments are in qualitative agreement with the theoretical analysis of Rudnick and Barmatz.[44]

V. CONCLUSION

We presented an apparatus to measure the oscillations of a levitated sphere in a single-axis acoustic levitator. In qualitative agreement with the existing theory, three types of levitation behavior were identified: stable, oscillation with constant amplitude and unstable levitation. When driven with constant frequency, the type of levitation behavior can be controlled by changing the distance between the emitter and the reflector. We also confirm that instabilities only occur when the driving frequency is higher than the resonance frequency of the levitator, leading to oscillations and potentially to the loss of the levitated sample. If necessary, these oscillations can be prevented either by changing the driving frequency or the distance between the emitter and the reflector.

SUPPLEMENTARY MATERIAL

See supplementary material for a video of the oscillational instability of the levitating sphere and a video of the sphere's vertical oscillation captured by a high-speed camera.

ACKNOWLEDGMENTS

This research was supported by the São Paulo Research Foundation – FAPESP (Grant No. 2017/27078-0) and by the European Union's Horizon 2020 research and innovation programme under the FET-Open Scheme with grant agreement No 737087. Gianluca Memoli's time is partially funded by his UKRI fellowship (EP/S001832/1).

REFERENCES

[1] E. H. Brandt, Nature **413**, 474 (2001).
[2] M. A. B. Andrade, N. Pérez, and J. C. Adamowski, Brazilian J. Phys. **48**, 190 (2018).
[3] H. Bruus, Lab Chip **12**, 1014 (2012).
[4] A. L. Yarin, M. Pfaffenlehner, and C. Tropea, J. Fluid Mech. **356**, 65 (1998).
[5] D. Zang, Y. Yu, Z. Chen, X. Li, H. Wu, and X. Geng, Adv. Colloid Interface Sci. **243**, 77 (2017).
[6] W. J. Xie and B. Wei, Phys. Rev. E - Stat. Nonlinear, Soft Matter Phys. **66**, 026605 (2002).
[7] S. Santesson and S. Nilsson, Anal. Bioanal. Chem. **378**, 1704 (2004).
[8] R. Tuckermann, L. Puskar, M. Zavabeti, R. Sekine, and D. McNaughton, Anal. Bioanal. Chem. **394**, 1433 (2009).
[9] R. Tuckermann, B. Neidhart, E. G. Lierke, and S. Bauerecker, Chem. Phys. Lett. **363**, 349 (2002).
[10] Y. Tian, R. G. Holt, and R. E. Apfel, Rev. Sci. Instrum. **66**, 3349 (1995).
[11] E. H. Trinh, P. L. Marston, and J. L. Robey, J. Colloid Interface Sci. **124**, 95 (1988).
[12] C. J. Benmore and J. K. R. Weber, Phys. Rev. X **1**, 011004 (2011).
[13] S. Tsujino and T. Tomizaki, Sci. Rep. **6**, 25558 (2016).
[14] W. J. Xie, C. D. Cao, Y. J. Lü, Z. Y. Hong, and B. Wei, Appl. Phys. Lett. **89**, 214102 (2006).
[15] D. Zang, K. Lin, L. Li, Z. Chen, X. Li, and X. Geng, Appl. Phys. Lett. **110**, 121602 (2017).
[16] C. T. Vi, A. Marzo, D. Ablart, G. Memoli, S. Subramanian, B. Drinkwater, and M. Obrist, in *Proc. 2017 ACM Int. Conf. Interact. Surfaces Spaces* (2017), pp. 161–170.
[17] S. Ueha, Y. Hashimoto, and Y. Koike, Ultrasonics **38**, 26 (2000).
[18] M. Takasaki, D. Terada, Y. Kato, Y. Ishino, and T. Mizuno, Phys. Procedia **3**, 1059 (2010).
[19] M. A. B. Andrade, A. L. Bernassau, and J. C. Adamowski, Appl. Phys. Lett. **109**, 044101 (2016).
[20] A. Marzo, S. A. Seah, B. W. Drinkwater, D. R. Sahoo, B. Long, and S. Subramanian, Nat. Commun. **6**, 8661 (2015).
[21] A. Marzo, M. Caleap, and B. W. Drinkwater, Phys. Rev. Lett. **120**, 044301 (2018).
[22] W. J. Xie and B. Wei, Appl. Phys. Lett. **79**, 881 (2001).
[23] M. A. B. Andrade, F. C. Buiochi, and J. Adamowski, IEEE Trans. Ultrason. Ferroelectr. Freq. Control **57**, 469 (2010).
[24] R. R. Whymark, Ultrasonics **13**, 251 (1975).
[25] C. R. Field and A. Scheeline, Rev. Sci. Instrum. **78**, 125102 (2007).
[26] E. H. Trinh, Rev. Sci. Instrum. **56**, 2059 (1985).
[27] J. K. R. Weber, C. A. Rey, J. Neuefeind, and C. J. Benmore, Rev. Sci. Instrum. **80**, 083904 (2009).
[28] A. Marzo, A. Barnes, and B. W. Drinkwater, Rev. Sci. Instrum. **88**, 085105 (2017).
[29] A. Ashkin and J. M. Dziedzic, Appl. Phys. Lett. **19**, 283 (1971).
[30] B. Z. Kaplan, Proc. Inst. Electr. Eng. **114**, 1801 (1967).
[31] D. Koyama and K. Nakamura, IEEE Trans. Ultrason. Ferroelectr. Freq. Control **57**, 1152 (2010).
[32] N. Bjelobrk, D. Foresti, M. Dorrestijn, M. Nabavi, and D. Poulikakos, Appl. Phys. Lett. **97**, 161904 (2010).
[33] D. Foresti, M. Nabavi, M. Klingauf, A. Ferrari, and D. Poulikakos, Proc. Natl. Acad. Sci. **110**, 12549 (2013).
[34] R. Kashima, D. Koyama, and M. Matsukawa, IEEE Trans. Ultrason. Ferroelectr. Freq. Control **62**, 2161 (2015).
[35] T. Hoshi, Y. Ochiai, and J. Rekimoto, Jpn. J. Appl. Phys. **53**, 07KE07 (2014).
[36] Y. Ochiai, T. Hoshi, and J. Rekimoto, PLoS One **9**, e97590 (2014).
[37] T. Omirou, A. Marzo, S. A. Seah, and S. Subramanian, in *Proc. 33rd Annu. ACM Conf. Hum. Factors Comput. Syst.* (2015), pp. 309–312.
[38] M. A. Norasikin, D. M. Plasencia, S. Polychronopoulos, G. Memoli, Y. Tokuda, and S. Subramanian, in *Proc. 31st ACM User Interface Softw. Technol. Symp. - UIST'18* (2018), pp. 247–259.
[39] E. H. Trinh and J. L. Robey, Phys. Fluids **6**, 3567 (1994).
[40] K. Hasegawa, Y. Abe, A. Kaneko, Y. Yamamoto, and K. Aoki, Microgravity Sci. Technol. **21**, S9 (2009).
[41] S. Baer, M. A. B. Andrade, C. Esen, J. C. Adamowski, G. Schweiger, and A. Ostendorf, Rev. Sci. Instrum. **82**, 105111 (2011).
[42] M. A. B. Andrade, N. Pérez, and J. C. Adamowski, J. Acoust. Soc. Am. **136**, 1518 (2014).
[43] N. Perez, M. A. B. Andrade, R. Canetti, and J. C. Adamowski, J. Appl. Phys. **116**, 184903 (2014).
[44] J. Rudnick and M. Barmatz, J. Acoust. Soc. Am. **87**, 81 (1990).
[45] E. Torres and A. Santillan, in *Proc. Acoust.* (2008).
[46] A. O. Santillán, R. R. Boullosa, V. Cutanda-Henríquez, and A. P. López, in *14th Int. Congr. Sound Vib.* (2007).
[47] A. Santillan, in *IEEE Int. Ultrason. Symp. IUS* (2011), pp. 1552–1555.
[48] D. Elleman, T. Wang, and M. Barmatz, *Acoustic Containerless Experiment System: A Non-Contact Surface Tension Measurement* (1988).
[49] P. C. Lin and I. Lin, Phys. Rev. E **93**, 021101 (2016).
[50] E. Leung, C. P. Lee, N. Jacobi, and T. G. Wang, J. Acoust. Soc. Am. **72**, 615 (1982).
[51] F. L. Curzon and D. Plant, Am. J. Phys. **54**, 367 (1986).
[52] M. Barmatz and P. Collas, Acoust. Soc. Am. **77**, 928 (1985).
[53] S. L. Garrett, *Understanding Acoustics: An Experimentalist's View of Acoustics and Vibration* (Springer, Cham, Switzerland, 2017).